Applied Analysis and Optimization
Volume 8, Number 3, 2024, 371–383

Yokohama Publishers
ISSN 2189-1664 Online Journal

ON THE DYNAMICS OF A DISCRETE RICCATI EQUATION WITH PERTURBATION

AHMED MOHAMMED AHMED EL-SAYED, SANAA MOUSSA SALMAN, AND MOSTAFA IBRAHIM

Abstract. In this paper, we discuss the new concept of a perturbation. As a simple example, we will study a discrete Riccati equation with perturbation to illustrate this concept. Analyses of the local stability of the fixed points and Neimark-Sacker bifurcation are presented. We use numerical simulations to draw out the results, as bifurcation diagrams, Lyapunov exponents, time series, and phase diagrams. This helps us confirm our research and unearth more complex dynamics.

1. Introduction

Dynamical systems theory is a mathematical framework that studies the behavior of systems as they evolve over time. It provides a powerful tool for modeling and understanding complex phenomena in various scientific disciplines, including physics, biology, economics, and engineering. Dynamical systems theory enables us to analyze the dynamic behavior of systems through differential equations, bifurcations, chaos theory, and stability analysis [10, 15, 16, 19, 21–25].

Chaos theory is a fascinating aspect of dynamical systems, focusing on systems that appear to exhibit random and unpredictable behavior. Chaos theory explores the underlying order and patterns in seemingly chaotic systems, emphasizing their sensitivity to initial conditions. It has profound implications for understanding complex systems in nature and society, such as weather patterns, population dynamics, and financial markets.

Bifurcation, a key concept in dynamical systems theory, refers to the qualitative change in the behavior of a system as a parameter is varied. Bifurcations can lead to the emergence of complex behavior, such as chaos, periodic orbits, or stable equilibria. Understanding bifurcations is essential for predicting and controlling system dynamics and exploring the boundaries between order and chaos.

By studying dynamical systems, chaos theory, and bifurcation, researchers and scientists can gain valuable insights into the intricate dynamics of natural and artificial systems. These concepts help us unravel the underlying principles governing complex phenomena and provide a deeper understanding of the world around us.

The discrete Riccati equation reads

$$\begin{aligned} x_{n+1} &= 1-\rho x_{n-1}^2, \qquad n=1,2,... \\ x(0) &= x_0,\ x(-1)=x_{-1}, \end{aligned} \tag{1.1}$$

2020 *Mathematics Subject Classification.* 34A12, 34K20, 34K27, 37C25, 37G15.
Key words and phrases. Riccati equation, discrete systems, perturbation, stability analysis, bifurcation.

where $\rho > 0$.

We can write equation (1.1) as a discrete system as follows

$$\begin{aligned} x_{n+1} &= 1 - \rho y_n^2, \\ y_{n+1} &= x_n, \\ x(0) &= x_0,\ y(0) = x_0 \end{aligned} \tag{1.2}$$

Let there exists a preturbation as

$$y_{n+1} = a x_n + \epsilon y_n.$$

The discrete Riccati equation with perturbation can considered as

$$\begin{aligned} x_{n+1} &= 1 - \rho y_n^2, \\ y_{n+1} &= a x_n + \epsilon y_n, \\ x(0) &= x_0\ ,\ y(0) = x_0, \end{aligned} \tag{1.3}$$

where $0 < \epsilon, a < 1$.

2. Local stability analysis

The local stability of the fixed points of (1.3) will be studied. The fixed points of the model can be acquired by solving the following system

$$\begin{aligned} x &= 1 - \rho y^2, \\ y &= a x + \epsilon y. \end{aligned} \tag{2.1}$$

Then, it is easy to see that the system has two fixed points (x_1^*, y_1^*) and (x_2^*, y_2^*) where

$$\begin{aligned} x_1^* &= -\frac{(\frac{1-\epsilon}{a})^2 + \sqrt{(\frac{1-\epsilon}{a})^4 + 4\rho(\frac{1-\epsilon}{a})}}{2\rho}, \\ y_1^* &= -\frac{(\frac{1-\epsilon}{a}) + \sqrt{(\frac{1-\epsilon}{a})^2 + 4\rho(\frac{1-\epsilon}{a})}}{2\rho}, \\ x_2^* &= -\frac{(\frac{1-\epsilon}{a})^2 - \sqrt{(\frac{1-\epsilon}{a})^4 + 4\rho(\frac{1-\epsilon}{a})}}{2\rho}, \\ y_2^* &= -\frac{(\frac{1-\epsilon}{a}) - \sqrt{(\frac{1-\epsilon}{a})^2 + 4\rho(\frac{1-\epsilon}{a})}}{2\rho}. \end{aligned}$$

The Jacobian matrix associated to the system (2.1) is given by

$$J(x, y) = \begin{bmatrix} 0 & -2\rho y \\ a & \epsilon \end{bmatrix}.$$

What follows is a stability analysis of fixed points.

2.1. **Stability analysis at** (x_1^*, y_1^*)**.** The Jacobian matrix calculated at (x_1^*, y_1^*) is given by

$$J(x_1^*, y_1^*) = \begin{bmatrix} 0 & -2\rho y_1^* \\ a & \epsilon \end{bmatrix}.$$

$J(x_1^*, y_1^*)$ has a characteristic equation given by

$$P(\lambda) \equiv \lambda^2 - \epsilon\lambda + \left[(\epsilon - 1) + \sqrt{(1-\epsilon)^2 + 4\rho a^2}\right] = 0.$$

To determine the local stability of the system (2.1) at the fixed point (x_1^*, y_1^*), the following lemmas is a useful tools.

Lemma 2.1. *Let $F(\lambda) = \lambda^2 + P\lambda + Q$ be the characteristic equation of eigen values associated to the Jacobin matrix evaluated at a fixed point(x^*, y^*) then (x^*, y^*) is*

1. *a sink if $\lambda_1 < 1$ and $\lambda_2 < 1$. That is a sink is locally stable,*
2. *a source if $\lambda_1 > 1$ and $\lambda_2 > 1$. That is a source is locally unstable,*
3. *a saddle if $\lambda_1 > 1$ and $\lambda_2 < 1$ or ($\lambda_1 < 1$ and $\lambda_2 > 1$),*
4. *a non hyperbolic if either $\lambda_1 = 1$ or $\lambda_2 = 1$.*

Lemma 2.2. *Let $F(\lambda) = \lambda^2 + P\lambda + Q$ suppose that $F(1) > 0$ and $F(\lambda) = 0)$ has two roots λ_1 and λ_2. then*

1. *$F(-1) > 0$ and $Q < 1$ if and only if $\lambda_1 < 1$ and $\lambda_2 < 1$,*
2. *$F(-1) < 0$ if and only if $\lambda_1 < 1$ and $\lambda_2 > 1$ or ($\lambda_1 > 1$ and $\lambda_2 < 1$),*
3. *$F(-1) > 0$ and $Q > 1$ if and only if $\lambda_1 > 1$ and $\lambda_2 > 1$.*

Depending on those lemmas, we find the following.

Theorem 2.3. *The fixed point (x_1^*, y_1^*) is stable if $0 < \rho < \frac{3-2\epsilon}{4a^2}$ and unstable if $\rho > \frac{3-2\epsilon}{4a^2}$.*

Proof.

$$J(x_1^*, y_1^*) = \begin{bmatrix} 0 & -2\rho y_1^* \\ a & \epsilon \end{bmatrix}.$$

The characteristic equation given by

$$\lambda^2 - \epsilon\lambda + 2a\rho y_1^* = 0,$$

$$\lambda^2 - \epsilon\lambda + 2a\rho\left[-\frac{(\frac{1-\epsilon}{a}) + \sqrt{(\frac{1-\epsilon}{a})^2 + 4\rho(\frac{1-\epsilon}{a})}}{2\rho}\right],$$

$$\lambda^2 - \epsilon\lambda + \left[(\epsilon - 1) + \sqrt{(1-\epsilon)^2 + 4\rho a^2}\right] = 0,$$

by applying lemmas [2.1, 2.2] we get

$$\left[(\epsilon - 1) + \sqrt{(1-\epsilon)^2 + 4\rho a^2}\right] < 1,$$

$$\sqrt{(1-\epsilon)^2 + 4\rho a^2} < 2 - \epsilon,$$

$$\rho < \frac{3 - 2\epsilon}{4a^2}.$$

The fixed point (x_1^*, y_1^*) is stable if $0 < \rho < \frac{3-2\epsilon}{4a^2}$ and unstable if $\rho > \frac{3-2\epsilon}{4a^2}$. $\square$

2.1.1. *Numerical simulations.* In this part, to validate our studies we use numerical experiments to draw out the theoretical results and show that changes in a and ϵ affect the dynamical behaviour of the dynamical system (2.1). We have been experimenting with different values of a and ϵ and then plotting bifurcation diagrams as a function of ρ. Moreover, the maximal Lyapunov exponent corresponding to each bifurcation diagram is introduced below it. In Figure (1a) we start with the initial point $(0.5, 0.4)$ at $a = 0.7,\ \epsilon = 0.1$ the system undergoes bifurcation at $\rho \simeq 1.42$. In Figure (1b) we start with the initial point $(0.5, 0.4)$ at $a = 0.7,\ \epsilon = 0.3$ the system undergoes bifurcation at $\rho \simeq 1.18$. In Figure (1e) we start with the initial point $(0.5, 0.4)$ at $a = 0.7,\ \epsilon = 0.0003$ the bifurcation occurs in the system at $\rho \simeq 1.5$. Figure (1f) illustrates that the bifurcation occurs in the system at $\rho \simeq 0.74$ with initial point $(0.5, 0.4)$ and $a = 0.9999,\ \epsilon = 0.00001$.

Also, we introduce some phase diagrams by taking $a = 0.7,\ \epsilon = 0.1$, and initial point $(0.5, 0.4)$ as in Figure (2). Through the increase in the value of ρ, the curve rotates clockwise and a period-4 orbit appears and the Lyapunov exponent becomes negative, as shown in Figures (2a)–(2g). The fixed point loses its stability and the curve turns into a limit cycle with an increase in radius and the Lyapunov exponent changes between negative and positive as in Figures (2h)–(2n). In Figure (2o) the limit cycle breaks down and a period-8 orbit appears and the Lyapunov exponent changes between negative and positive. The system becomes more chaotic and the Lyapunov exponent becomes positive as in Figure (2p).

Moreover, we introduce time series at the initial point $(0.5, 0.4)$ with the same values of a and ϵ in Figure (3)

2.2. **Stability analysis at** (x_2^*, y_2^*)**.** The Jacobian matrix calculated at (x_2^*, y_2^*) is given by

$$J(x_2^*, y_2^*) = \begin{bmatrix} 0 & -2\rho y_2^* \\ a & \epsilon \end{bmatrix}.$$

$J(x_2^*, y_2^*)$ has a characteristic equation given by

$$P(\lambda) \equiv \lambda^2 - \epsilon\lambda + 2a\rho\left[-\frac{(\frac{1-\epsilon}{a}) - \sqrt{(\frac{1-\epsilon}{a})^2 + 4\rho(\frac{1-\epsilon}{a})}}{2\rho}\right] = 0.$$

To determine the local stability of the system (2.1) at the fixed point (x_2^*, y_2^*), Depending on previous lemmas, we find the following.

Theorem 2.4. *The fixed point* (x_2^*, y_2^*) *is stable if* $0 < \rho < \frac{3-2\epsilon}{4a^2}$ *and unstable if* $\rho > \frac{3-2\epsilon}{4a^2}$.

Proof.

$$J(x_2^*, y_2^*) = \begin{bmatrix} 0 & -2\rho y_2^* \\ a & \epsilon \end{bmatrix}.$$

The characteristic equation given by

$$\lambda^2 - \epsilon\lambda + 2a\rho y_2^* = 0,$$

$$\lambda^2 - \epsilon\lambda + 2a\rho\Big[- \frac{(\frac{1-\epsilon}{a}) - \sqrt{(\frac{1-\epsilon}{a})^2 + 4\rho(\frac{1-\epsilon}{a})}}{2\rho}\Big],$$

$$\lambda^2 - \epsilon\lambda + \big[- (1-\epsilon) - \sqrt{(1-\epsilon)^2 + 4\rho a^2}\big] = 0,$$

by applying lemmas [2.1, 2.2] we get

$$-\big[(1-\epsilon) - \sqrt{(1-\epsilon)^2 + 4\rho a^2}\big] < 1,$$

$$\sqrt{(1-\epsilon)^2 + 4\rho a^2} < 2 - \epsilon,$$

$$\rho < \frac{3-2\epsilon}{4a^2}.$$

The fixed point (x_2^*, y_2^*) is stable if $0 < \rho < \frac{3-2\epsilon}{4a^2}$ and unstable if $\rho > \frac{3-2\epsilon}{4a^2}$. □

2.2.1. *Numerical simulations.* In this part, to validate our studies we use numerical experiments to draw out the theoretical results and show that changes in a and ϵ affect the dynamical behaviour of the dynamical system (2.1). We have been experimenting with different values of a and ϵ and then plotting bifurcation diagrams as a function of ρ. Moreover, the maximal Lyapunov exponent corresponding to each bifurcation diagram is introduced below it. In Figure (4a) we start with the initial point $(0.2, 0.2)$ at $a = 0.7,\ \epsilon = 0.1$ the system undergoes bifurcation at $\rho \simeq 1.42$. In Figure (4b) we start with the initial point $(0.2, 0.2)$ at $a = 0.7,\ \epsilon = 0.3$ the system undergoes bifurcation at $\rho \simeq 1.18$. In Figure (4e) we start with the initial point $(0.2, 0.2)$ at $a = 0.7,\ \epsilon = 0.0003$ the bifurcation occurs in the system at $\rho \simeq 1.5$. Figure (4f) illustrates that the bifurcation occurs in the system at $\rho \simeq 0.74$ with initial point $(0.2, 0.2)$ and $a = 0.9999,\ \epsilon = 0.00001$.

Also, we introduce some phase diagrams by taking $a = 0.7$, $\epsilon = 0.1$, and initial point $(0.2, 0.2)$ as in Figure (5). Through the increase in the value of ρ, the curve rotates clockwise and a period-4 orbit appears and the Lyapunov exponent becomes negative, as shown in Figures (5a)–(5f). The fixed point loses its stability and the curve turns into a limit cycle with an increase in radius and the Lyapunov exponent changes between negative and positive as in Figures (5g)–(5n). In Figure (5o) the limit cycle breaks down and a period-8 orbit appears and the Lyapunov exponent changes between negative and positive. The system becomes more chaotic and the Lyapunov exponent becomes positive as in Figure (5p).

Moreover, we introduce time series at the initial point $(0.2, 0.2)$ with the same values of a and ϵ in Figure (5).

3. Conclusion

In this study, a Riccati equation with a perturbation parameters was studied. We looked at both the solution's existence and its continuous dependence on the initial conditions. Analyses of Hopf bifurcations and fixed points' local stability were presented.. local stability of fixed points were studied. We validated our results using numerical simulations that generated bifurcation diagrams, Lyapunov exponents, time series, and phase diagrams to better understand the underlying complicated dynamics, it has been shown that, when the perturbation parameters is increased, chaos is advanced in the system's dynamics

References

[1] P. Acquistapace and F. Bucci, *Uniqueness for Riccati equations with application to the optimal boundary control of composite systems of evolutionary partial differential equations*, Annali di Matematica Pura ed Applicata (2023).

[2] M. U. Akhmet, D. Altntana and T. Ergenc, *Chaos of the logistic equation with piecewise constant arguments*, arXiv preprint arXiv:1006.4753 (2010).

[3] B. D. Anderson, J. B. Moore, *Optimal Control-linear Quadratic Methods*, Courier Corporation, 2007.

[4] B. D. O. Anderson and J. B. Moore, *Linear Optimal Control*, Prentice-Hall, Englewood Cliffs, NJ, 1971.

[5] S. Aubry and P.Y. Le Daeron, *The discrete Frenkel-Kontorova model and its extensions I*, Physica D **8** (1983), 381–422.

[6] J. Baumeister, A. Leitao and G. N. Silva, *On the value function for nonautonomous optimal control problem with infinite horizon*, Systems Control Lett. **56** (2007), 188–196.

[7] J. Blot, *Infinite-horizon Pontryagin principles without invertibility*, J. Nonlinear Convex Anal. **10** (2009), 177–189.

[8] J. Blot and P. Cartigny, *Optimality in infinite-horizon variational problems under sign conditions*, J. Optim. Theory Appl. **106** (2000), 411–419.

[9] J. F. Carinena, G. Marmo, A. M. Perelomov and M. F. Z. Ranada, *Related operators and exact solutions of Schr 旦 dinger equations*, International Journal of Modern Physics A **13** (1998), 4913–4929.

[10] A. M. A. El-Sayed, A. Elsaid, H. M. Nour and A. Elsonbaty, *Dynamical behavior, chaos control and synchronization of a memristor-based ADVP circuit*, Commun. Nonlinear Sci. Numer. Simul. (2012).

[11] A. M. A. El-Sayed and S. M. Salman, *Chaos and bifurcation of discontinuous dynamical systems with piecewise constant arguments*, Malaya Journal of Matematik **1** (2012), 14–18.

[12] A. M. A. El-Sayed and S. M. Salman, *Chaos and bifurcation of the Logistic discontinuous dynamical systems with piecewise constant arguments*, Malaya Journal of Matematik **3** (2013), 14–20.

[13] A. M. A. El-Sayed, S. M. Salman, *On a discretization process of fractional-order Riccati differential equation*, J. Fract. Calc. Appl **4** (2013), 251–259.

[14] A. M. A. El-Sayed, S. M. Salman, A. A. F. AbdElfattah, *On the dynamics of a Riccati differential equation with perturbed delay*, Electronic Journal of Mathematical Analysis and Applications **11** (2023), 1–14.

[15] R. A. Frantz, J. C. Loiseau and J. C. Robinet, *Krylov methods for large-scale dynamical systems: Application in fluid dynamics*, App. Mech. Rev. (2023).

[16] K. Gajamannage, D. I. Jayathilake, Y. Park and E. M. Bollt, *Recurrent neural networks for dynamical systems: Applications to ordinary differential equations, collective motion, and hydrological modeling*, Chaos **33** (2023).

[17] J. K. Hale, E. F. Infante and F. S. Tsen, *Stability in linear delay equations*, Journal of Mathematical Analysis and Applications **105** (1985), 533–555.

[18] G. Mönnel, M. Siebert, C. Brendle and P. Rostalski, *Robust model predictive control of an anaesthesia workstation ventilation unit* at-Automatisierungstechnik **68** (2020).

[19] L. Kocarev, S. Lian, *Chaos-Based Cryptography*, Springer, 2011.

[20] W. T. Reid, *Riccati Differential Equations*, Mathematics in Science and Engineering, vol. 86, Academic Press, 1972.

[21] S. H. Strogatz, *Nonlinear Dynamics and Chaos with Applications to Physics, Biology, Chemistry, and Engineering*, CRC press, 2018.

[22] P. N. V. Tu, *Dynamical Systems: An Introduction with Applications in Economics and Biology*, Springer Science & Business Media, 2012.

[23] S. Vaidyanathan and K. Rajagopal, *LabVIEW implementation of chaotic masking with adaptively synchronised forced Van der Pol oscillators and its application in real-time image encryption*, Int. J. of Simulation and Process Modelling **12** (2017), 165–178.

[24] N. Yadav, S. Ravela and A. R. Ganguly, *Machine learning for robust identification of complex nonlinear dynamical systems: applications to earth systems modeling*, arXiv preprint arXiv:2008.05590 (2020).

[25] C. Zhu, *A novel image encryption scheme based on improved hyperchaotic sequences*, Opt. comm. **285** (2012), 29–37.

Manuscript received June 1 2024
revised September 3 2024

A. M. A. El-Sayed
Alexandria, Egypt
E-mail address: amasayed@alexu.edu.eg

S. M. Salman
Alexandria, Egypt
E-mail address: samastars9@alexu.edu.eg

M. Ibrahim
Alexandria, Egypt
E-mail address: mostafaibrahim11mo@gmail.com

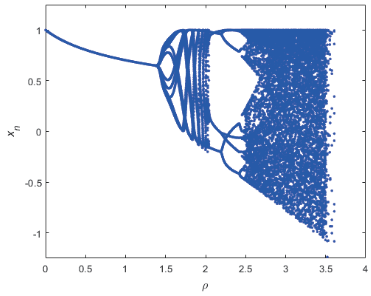

(A) $a = 0.7$, $\epsilon = 0.1$

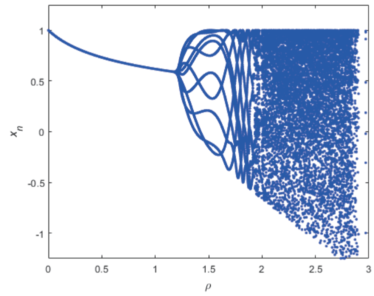

(B) $a = 0.7$, $\epsilon = 0.3$

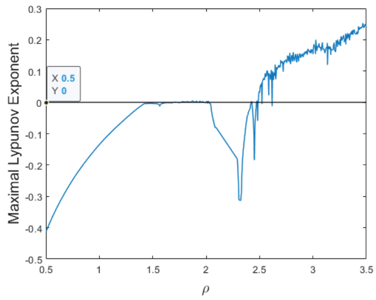

(C) $a = 0.7$, $\epsilon = 0.1$

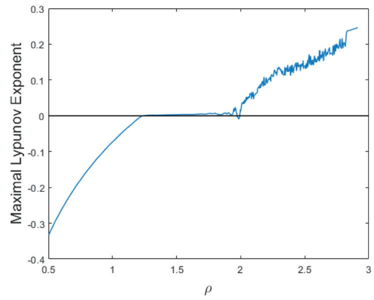

(D) $a = 0.7$, $\epsilon = 0.3$

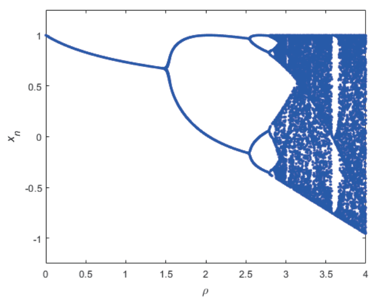

(E) $a = 0.7$, $\epsilon = 0.0003$

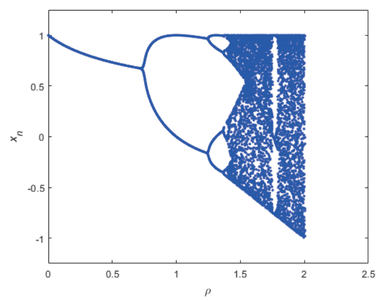

(F) $a = 0.9999$, $\epsilon = 0.00001$

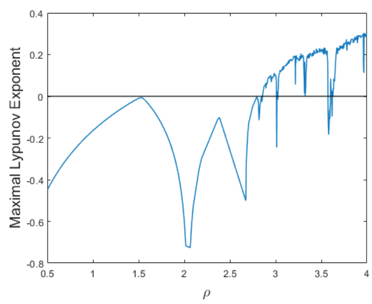

(G) $a = 0.7$, $\epsilon = 0.0003$

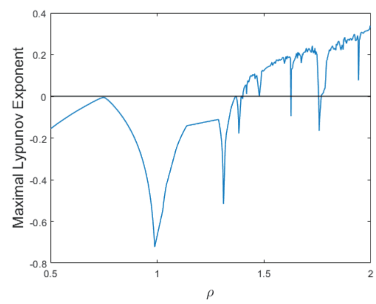

(H) $a = 0.9999$, $\epsilon = 0.00001$

FIGURE 1. Bifurcation diagrams of a system (2.1) and its accompanying maximum Lyapunov exponent

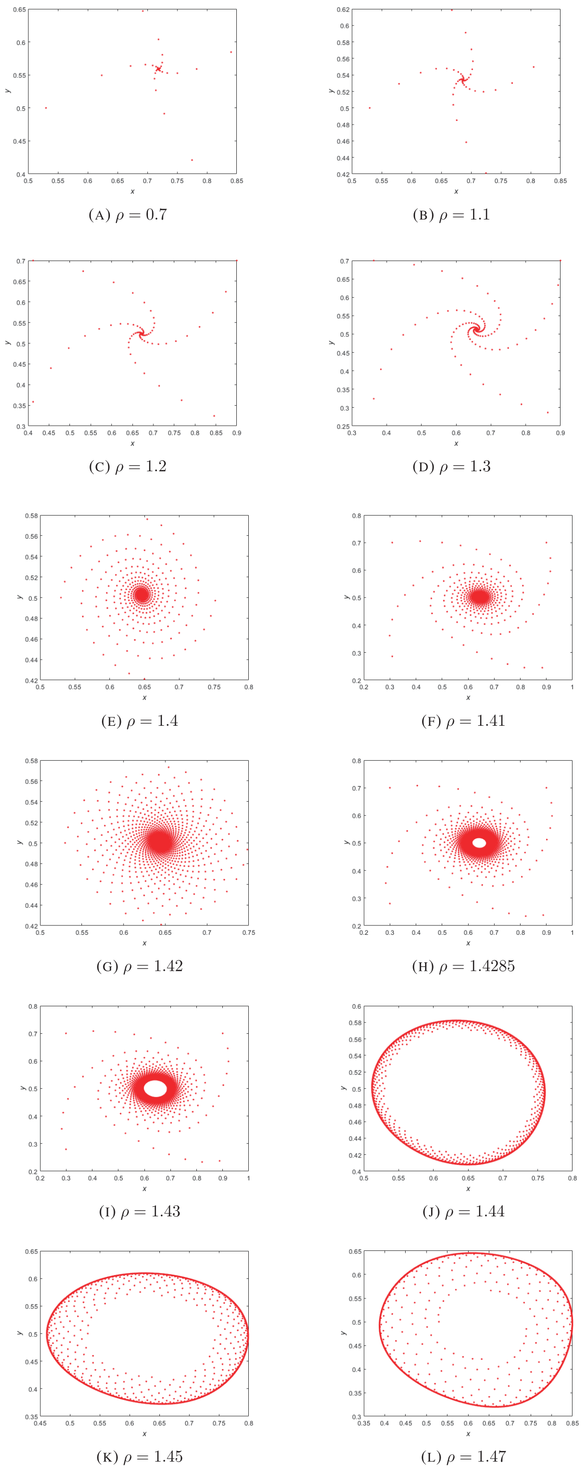

(A) $\rho = 0.7$ (B) $\rho = 1.1$

(C) $\rho = 1.2$ (D) $\rho = 1.3$

(E) $\rho = 1.4$ (F) $\rho = 1.41$

(G) $\rho = 1.42$ (H) $\rho = 1.4285$

(I) $\rho = 1.43$ (J) $\rho = 1.44$

(K) $\rho = 1.45$ (L) $\rho = 1.47$

FIGURE 2. Phase diagrams of system (2.1) with varying values of ρ

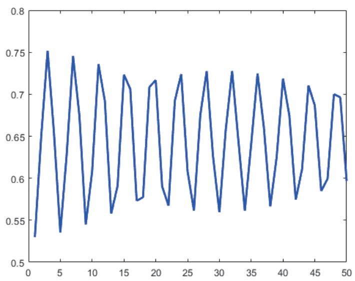

(A) a= 0.7 esp =0.1

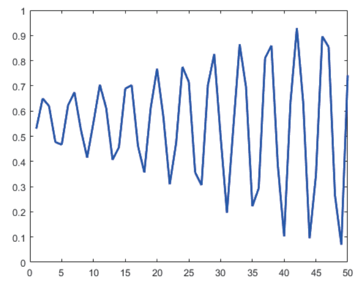

(B) a = 0.7 esp 0.3

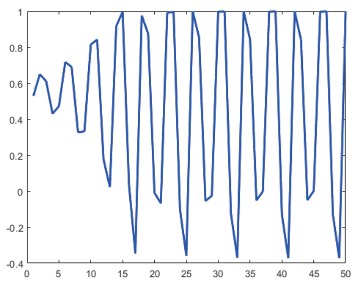

(C) a = 0.9 esp 0.3

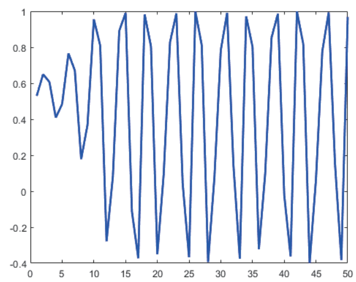

(D) a = 0.9999 eps = 0.00001

FIGURE 3. Time series of system (2.1)

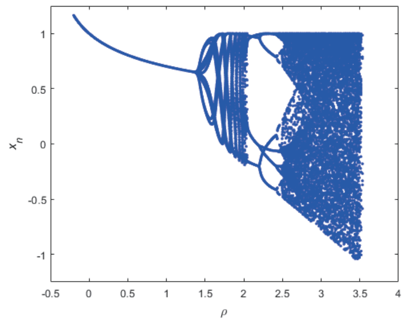

(A) $a = 0.7$, $\epsilon = 0.1$

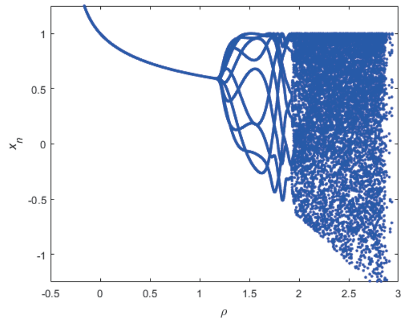

(B) $a = 0.7$, $\epsilon = 0.3$

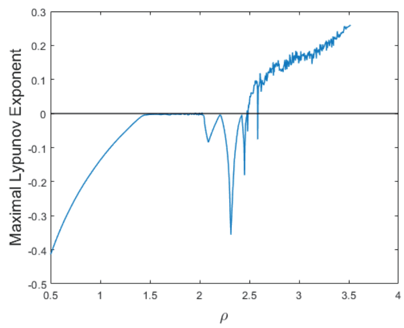

(C) $a = 0.7$, $\epsilon = 0.1$

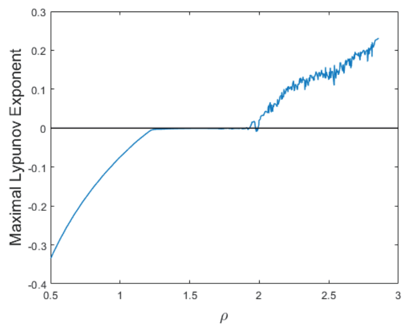

(D) $a = 0.7$, $\epsilon = 0.3$

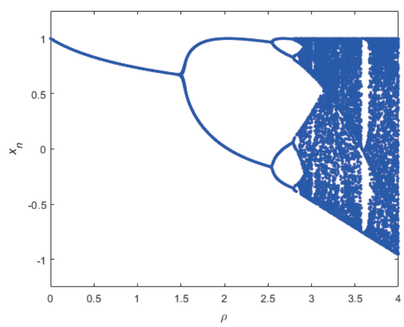

(E) $a = 0.7$, $\epsilon = 0.0003$

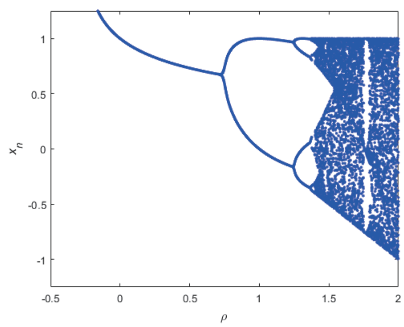

(F) $a = 0.9999$, $\epsilon = 0.00001$

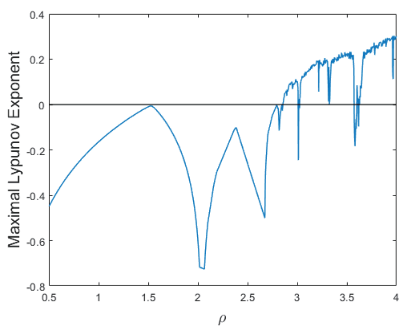

(G) $a = 0.7$, $\epsilon = 0.0003$

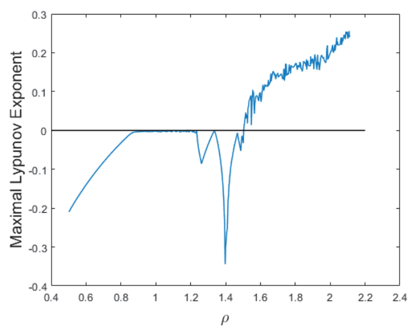

(H) $a = 0.9999$, $\epsilon = 0.00001$

FIGURE 4. Bifurcation diagrams of a system (2.1) and its accompanying maximum Lyapunov exponent

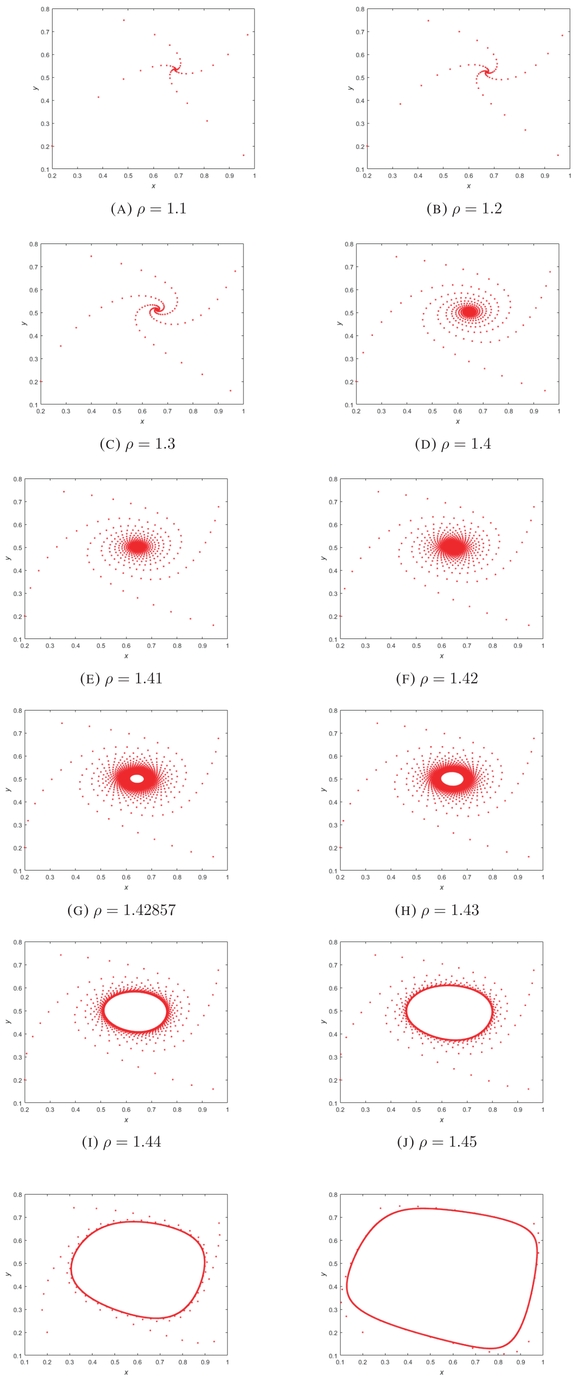

(A) $\rho = 1.1$ (B) $\rho = 1.2$

(C) $\rho = 1.3$ (D) $\rho = 1.4$

(E) $\rho = 1.41$ (F) $\rho = 1.42$

(G) $\rho = 1.42857$ (H) $\rho = 1.43$

(I) $\rho = 1.44$ (J) $\rho = 1.45$

(K) $\rho = 1.5$ (L) $\rho = 1.6$

FIGURE 5. Phase diagrams of system (2.1)with varying values of ρ

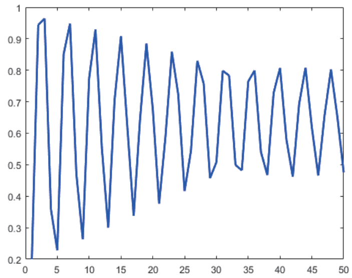

(Q) a =0.7 eps =0.1

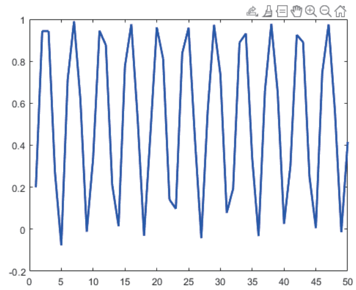

(R) a = 0.7 eps = 0.3

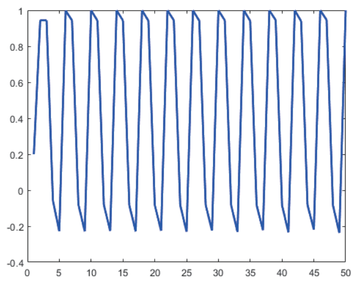

(S) a = 0.9 eps = 0.1

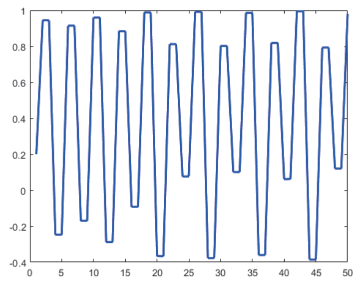

(T) a = 0.9999 eps = 0.00001

FIGURE 6. time series of system(2.1)